Atmospheric Environment 156 (2017) 95–101

Contents lists available at ScienceDirect

Atmospheric Environment

journal homepage: www.elsevier.com/locate/atmosenv

Elevated production of NH_4NO_3 from the photochemical processing of vehicle exhaust: Implications for air quality in the Seoul Metropolitan Region

Michael F. Link [a], Jounghwa Kim [b], Gyutae Park [c], Taehyoung Lee [c], Taehyun Park [c], Zaeem Bin Babar [d], Kijae Sung [b], Pilho Kim [c], Seokwon Kang [c], Jeong Soo Kim [b], Yongjoo Choi [c], Jihawn Son [b, *], Ho-Jin Lim [d], Delphine K. Farmer [a]

[a] Department of Chemistry, Colorado State University, Fort Collins 80523, CO, United States
[b] Transportation Pollution Research Center, National Institute of Environmental Research, Incheon, South Korea
[c] Department of Environmental Science, Hankuk University of Foreign Studies, Yongin, South Korea
[d] Department of Environmental Engineering, Kyungpook National University, Daegu, South Korea

HIGHLIGHTS

- Elevated NH_4NO_3 formation from photochemical perturbation of vehicle exhaust.
- NH_3, emitted from TWCs, limits the formation of NH_4NO_3 in NO_x-saturated diesel exhaust.
- Vehicles with TWCs could make important contributions to NH_4NO_3 pollution in the SMR.

ARTICLE INFO

Article history:
Received 5 October 2016
Received in revised form
16 February 2017
Accepted 18 February 2017
Available online 27 February 2017

Keywords:
Ammonium nitrate
Vehicular ammonia
Vehicle exhaust photochemical oxidation
Korean air quality

ABSTRACT

A vehicle fleet representative of passenger vehicles driven in the Seoul Metropolitan Region was investigated for primary emissions and secondary chemistry. Exhaust was photochemically oxidized in a flow reactor to determine the ammonium nitrate (NH_4NO_3) aerosol formation potential from vehicles of gasoline, diesel and liquid petroleum gasoline (LPG) fuel types. Secondary formation of aerosol NH_4NO_3, was larger than primary emissions for all vehicle fuel types except diesel, for which negligible secondary NH_4NO_3 production was observed. Although diesel vehicles emitted more primary nitrogen oxides than other vehicle types, ammonia emitted from gasoline and liquid petroleum gasoline fuels types limited the secondary production of NH_4NO_3. The results suggest that gasoline and liquid petroleum gasoline vehicles with three-way catalysts could be an important source of ammonia for NH_4NO_3 aerosol formation in ammonia-limited environments, including the Seoul Metropolitan Region.

1. Introduction

Measured fine particle burdens in the Seoul Metropolitan Region (SMR) are high despite ongoing efforts by the Korean Ministry of the Environment, including the enactment of the "Special Act on Metropolitan Air Quality Improvement" more than a decade ago. The particle burdens are similar to other large Asian cities such as Tokyo (Heo et al., 2009; Shin et al., 2012) and Shanghai (Chang et al., 2015), and are responsible for low visibility and decreased air quality. The SMR, which includes Incheon, Seoul, and parts of the Gyeonggi province, includes multiple pollution sources including biomass burning, industry, vehicles/transportation, and long-range transport. However, the exact contribution of each of these sources to observed fine particulate matter ($PM_{2.5}$) in the area is poorly understood (Heo et al., 2009; Kim, 2007). Effective policy that reduces air pollution and human exposure to $PM_{2.5}$ in the SMR requires an understanding of how different sources contribute precursors to secondary $PM_{2.5}$ and thus local air pollution (Aksoyoglu et al., 2016; Huang et al., 2014).

Severe haze events in highly populated cities are dominantly due to secondary aerosol production (Guo et al., 2014; Wang et al., 2016). In these events, the inorganic aerosol component often

* Corresponding author.
E-mail address: riverever@korea.kr (J. Son).

http://dx.doi.org/10.1016/j.atmosenv.2017.02.031
1352-2310/

contributes to the total observed particle mass equally or greater than the organic fraction (Huang et al., 2014; Park et al., 2013; Petetin et al., 2016). Vehicles in megacities can play an important role in these localized haze events by emitting nitrogen oxides (NO_x) that photochemically form nitric acid (HNO_3), leading to secondary inorganic ammonium nitrate (NH_4NO_3) through thermodynamic equilibrium with gas-phase ammonia (NH_3) (Chang et al., 2015; Wang et al., 2013). Introduction of stringent standards for vehicle emissions (such as the EURO 6 for diesel vehicles and California's non-methane organic gases fleet average system for gasoline-fueled vehicles; NMOG FAS) have been largely credited with reducing NO_x and non-methane volatile organic compounds throughout South Korea over the last twenty years (Park et al., 2013). However, ozone concentrations in the SMR have continued to increase, and visibility has continued to decrease, since 1989 (the start of the air quality monitoring network) (Shin et al., 2012). Previous studies suggest that a strong photochemical aerosol component contributes to localized air pollution in the SMR (Heo et al., 2009; Kim, 2007).

Vehicles with a three-way catalyst system (TWC) produce NH_3 through a water gas-shift reaction on the catalyst involving carbon monoxide (CO), hydrogen gas and nitrogen monoxide (NO) (Behera et al., 2013; Grenoble et al., 1981; Livingston et al., 2009; Suarez-Bertoa et al., 2014). These TWCs are commonly used for gasoline and liquid petroleum gasoline (LPG) fuel types. In contrast, diesel vehicles are not equipped with TWCs and thus, unless equipped with modern NO_x-mitigating systems such as the selective catalytic reduction system, are unimportant sources of NH_3 to the urban atmosphere (Suarez-Bertoa et al., 2015; Suarez-Bertoa and Astorga, 2016a). As of May 2016, vehicles equipped with the TWC system and powered by gasoline or LPG comprise over 60% of the total on-road vehicle fleet in Seoul (Ministry of Land, Infrastructure, and Transport, 2016) and thus represent a potentially important source of NH_3 for NH_4NO_3 aerosol formation. Evidence of high fractions of aerosol nitrate have been observed from particle pollution events in and around the SMR (Choi et al., 2001; Geng et al., 2011; Kim, 2007; Park et al., 2013), as well as in air transported downwind of the SMR (>30% of particle mass) during times of morning traffic. These observations suggest that photochemically processed vehicle emissions contribute to localized PM pollution from the SMR (Lee et al., 2016). Here, we use a flow reactor study to investigate the hypothesis that NH_3 formed inside the catalytic converters of gasoline and LPG vehicles rapidly reacts with HNO_3 derived from NO_x to act as the dominant source of NH_4NO_3 in the SMR. Additionally, we observe very low NH_4NO_3 formation from NO_x-saturated diesel exhaust, suggesting that NH_3 is the limiting reagent for NH_4NO_3 production from engine exhaust, and that controlling NH_3 emissions from gasoline and LPG vehicles may be key to reducing secondary inorganic aerosol in NO_x-dominant ambient environments, including the SMR.

2. Materials and methods

2.1. Vehicle exhaust sampling

Vehicle exhaust sampling was conducted at the Transportation Pollution Research Center (TPRC) of the National Institute of Environmental Research (NIER), a certifying institute for vehicle exhaust emissions in Korea. The specifications for the vehicles tested are shown in Table 1. Four gasoline (G1-4), three diesel (D1-3), and three liquid petroleum gasoline (LPG; L1-3) vehicles were chosen as a representative fleet of SMR vehicles.

Testing for each vehicle required two days. Experiments took place between 18 November 2015 and 22 July 2016. Emissions were generated from vehicles operated under 20-min constant speed driving conditions using a chassis dynamometer. Vehicle exhaust was diluted in a constant volume sampler with dilution ratios ranging from 10 to 60 (clean air/exhaust). Diluted air was pumped through 6 m of stainless steel tubing (3/8″ O.D.) connected to a 1 m length of stainless steel tubing (1/4" O.D.) at a flowrate of 3 standard liters per minute (sLpm). During the 20-min constant speed driving mode, the sampled air would pass through an oxidation flow reactor (KNU OFR) and either be transferred to the HR-AMS, or transferred to a bypass every 2 min. This sampling design allowed the exhaust sample a greater opportunity to equilibrate in the flow reactor than if the diluted sample alternated through the KNU OFR and a bypass line. Primary emissions were measured by pumping undiluted exhaust through a separate line (2 m of stainless steel tubing) at a flowrate of 3 sLpm while the diluted air was diverted through the OFR bypass.

2.2. Emissions measurement information

Measurements of NO, NO_2, and NH_3 were acquired using a Horiba MEXA 1400QL-NX analyzer. NO_x was measured by chemiluminescence; CO and CO_2 were measured by non-dispersive infrared detectors. The authors note that measurements of NH_3 were only available for vehicles D1, G2, and L3 and were acquired several months after measurements that included the OFR were performed. All emissions tests were performed in accordance with

Table 1
Specifications of the vehicle population tested at the TPRC separated by fuel type and brand.

[a]Vehicle ID	Brand	Fuel	After-treatment	Fuel delivery	Engine displacement (cc)	Odometer (km)	Emission standard
D1	A	Diesel	[b]DOC + [c]DPF	[e]DI	1582	15,396	Euro 6
G2	A	Gasoline	[d]TWC	[f]GDI	1591	71,480	ULEV
L3	A	LPG	TWC	[g]LPI	1591	54,930	ULEV
D4	B	Diesel	DOC + DPF	DI	2199	54,060	Euro 6
G5	B	Gasoline	TWC	GDI	2999	26,800	ULEV
L6	B	LPG	TWC	LPI	2999	43,784	ULEV
G7	C	Gasoline	TWC	GDI	1999	29,560	ULEV
L8	C	LPG	TWC	LPI	1999	37,268	ULEV
D9	D	Diesel	DOC + DPF	DI	1956	17,870	Euro 5
G10	E	Gasoline	TWC	GDI	998	51,914	ULEV

[a] Vehicle IDs beginning with G are for gasoline, D are for diesel and L are for LPG.
[b] Diesel oxidation catalyst (DOC).
[c] Diesel particle filter (DPF).
[d] Three way catalyst (TWC).
[e] Direct injection (DI).
[f] Gasoline direct injection (GDI).
[g] Liquid phase injection (LPI).

the World Forum for Harmonization of Vehicle Regulations, an international standard method used by the United Nations Economic Commission for Europe (UNECE). The Constant Volume Sampling method recommended by UNECE for hot-start was performed by running the engine until the engine temperature is the half of temperature gauge. This generally took 5–10 min. After the engine temperature reached the halfway point on the temperature gauge, the test vehicle was run for a distance of 4 km at a speed of 70 km/h. The vehicle then would slow down to 30 km/h (the first testing speed) and emissions measurements would then begin.

2.3. Flow reactor operation

We used a custom-built oxidation flow reactor (Kyungpook National University OFR; KNU OFR) to observe the formation of secondary inorganic aerosol from samples of vehicle exhaust. The KNU OFR was similar in its design to previously described flow reactors (Chhabra et al., 2015; Friedman et al., 2016; Lambe et al., 2015, 2011), and consisted of a pyrex quartz tube 80 cm in length with an inner diameter of 14.3 cm. OH radicals were produced by introducing O_3 to the sample flow which was photolyzed ($\lambda = 254$ nm) in the reactor to form OH radicals. An OH exposure calibration was performed over the range of lamp operating voltages; OH exposures ranged from 6.5×10^{10} to 6.5×10^{11} molecules cm^{-3} s, corresponding to 0.5–5 days of OH equivalent atmospheric processing (assuming an average OH concentration of 1×10^6 molecules cm^{-3}). An analysis presented in the supporting information suggests the measurements from vehicles G2, L3, G7, L8, D9 and G10 should reflect OH exposures on the lower end of the calibrated range; approximately 0.5–1 days of OH equivalent atmospheric processing. The OH exposure for L6 may be higher than the other vehicles, and the OH exposure for D1 and D4 should be similar to or lower than the other vehicles.

The authors recognize recent modeling studies analyzing OFR oxidation chemistry as a function of relative humidity, photon flux, input ozone and externally added OH reactivity (Li et al., 2015; Peng et al., 2016, 2015). The conclusions of Peng et al. (2016) define the interpretation of OFR results as “risky” when either the water vapor mixing ratio is <0.1% or when the externally added OH reactivity is > 200 s^{-1}. Experiments using an OFR to explore the photochemical oxidation potential of vehicle exhaust and biomass burning commonly are operated under “riskier” conditions due to the presence of near-ppm levels of NO_x and/or high levels of reactive VOCs in the reactor (Jathar et al., 2017; Karjalainen et al., 2016; Link et al., 2016; Ortega et al., 2013; Tkacik et al., 2014). Ultimately, the effect of high externally added OH reactivity in the OFR is that, particularly for VOCs, the potential effects of photolysis and non-OH oxidation chemistry become increasingly uncertain (Peng et al., 2016). The analytical challenge of characterizing the photochemical oxidation of either vehicle exhaust or biomass burning as it occurs in the ambient environment through the use of OFRs remains and should be the subject of future study.

2.4. High resolution time-of-flight aerosol mass spectrometer (HR-AMS)

The Aerodyne HR-AMS has been described extensively in previous literature, and details of its operation will be briefly described here (DeCarlo et al., 2006; Kuwayama et al., 2015; Middlebrook et al., 2012). The exhaust sample passed through a diffusion drier and critical orifice, restricting the flow to 0.1 Lpm before entering the HR-AMS. Diffusion dryers controlled sample humidity (<40% RH), reducing uncertainties due to bounce-related changes in collection efficiency and reduced particle transmission through the aerodynamic lens (Middlebrook et al., 2012). The HR-AMS was calibrated weekly and the Composition-Dependent Collection Efficiency (CDCE) was calculated from observed chemical composition. Only low-humidity experiments were used for quantitative HR-AMS analysis. Data were collected at 10s resolution.

3. Results and discussion

3.1. Trace gas and inorganic particle data

Here we present the primary emissions in terms of a distance-based emission factor. We express the inorganic aerosol produced from photochemical perturbation of the primary exhaust in terms of a photochemically enhanced (P.E.) distance-based emission factor. The P.E. emission factor is defined as the effective emission factor of a given compound after the vehicle exhaust has been exposed to 0.5–1 day of OH equivalent atmospheric aging. Throughout the sampling campaign, production of secondary inorganic aerosol in the form of NH_4NO_3 was most pronounced from vehicles fueled by gasoline and LPG (Fig. 1).

In contrast, emissions of primary inorganic aerosol (PIA) were close to the HR-AMS detection limits for all fuel types. We observed higher levels of secondary aerosol ammonium and nitrate than sulfate across all fuel types. Some vehicles (e.g. D4 and G10) show elevated nitrate P.E. emission factors associated with influences of speed on engine performance (Fig. 2 and Fig. S5).

The results indicate that relatively small amounts of photochemical perturbation can produce secondary aerosol from gaseous precursors in the exhaust. This secondary aerosol can be more than an order of magnitude greater than primary aerosol emissions. This is consistent with previous studies (Liu et al., 2016), including measurements of gasoline exhaust oxidation in a smog chamber (Nordin et al., 2013). Higher levels of CO were associated with higher NH_4NO_3 emission and production. In contrast, higher levels of NO_x were not correlated with higher levels of NH_4NO_3. Higher levels of CO emissions from gasoline vehicles often coincide with higher levels of NH_3 emissions (Livingston et al., 2009; Suarez-Bertoa et al., 2014). In this study, we observe elevated NH_4NO_3 production corresponding to elevated CO emissions, suggesting that CO is an appropriate proxy measurement for NH_3 from gasoline and LPG vehicles in this study. The diesel particle filter (DPF) and diesel oxidation catalyst (DOC) are often used as exhaust aftertreatment technologies in diesel vehicles. However, these aftertreatments fail to remove NO_x, causing higher NO_x emissions from diesel than gasoline vehicles. The limiting reagent for NH_4NO_3 formation can be either NO_x or NH_3, depending on the ambient environment. Both gasoline/LPG vehicles and diesel vehicles can act as a source of the limiting reactant, and spur secondary inorganic aerosol formation. The observations described herein demonstrate that in an NH_3-limited environment, gasoline and LPG vehicles can provide NH_3 and thus cause increased particulate matter loading, while in a NO_x-limited environment, diesel vehicles can provide the NO_x to produce particles.

Photochemically enhanced emission factors of inorganic aerosol from the gasoline and LPG fuel types vary widely by car brand (Fig. 3). These differences can be attributed to engine design, combustion conditions and chemistry, as well as driving speed (e.g. Fig. 2). Fig. 3 shows the relationship between the different cars from which exhaust was sampled, and the production of aerosol nitrate.

Vehicles G2, L3, and G7 all have median values for secondary nitrate P.E. emission factors that are much higher than other vehicle brands. Vehicles G5 and L8 have median values for secondary nitrate production that are much lower than G2, L3 and G7, but still a factor of 5 or more higher than the diesel vehicles (D1, D4, and D9) as well as L6 and G10. The vehicles that were observed to have the highest secondary aerosol production rates were G2 and L3.

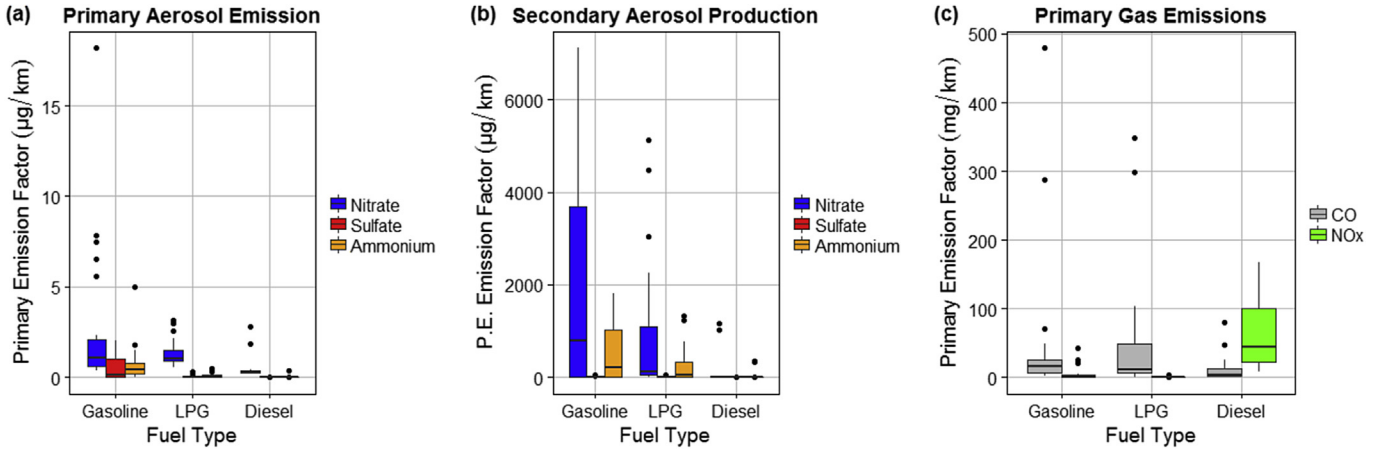

Fig. 1. Inorganic aerosol and gas emission factors measured as (a) primary aerosol emission, (b) secondary aerosol production after oxidation in the KNU OFR and (c) primary gas emission. The edges of the boxplots represent the 25th and 75th quartiles and the whiskers represent the 10th and 90th quartiles. The median value is represented by the solid black lines in the boxes (N = 21 for diesel, N = 24 for LPG, and N = 27 for gasoline). Outliers are shown as black dots.

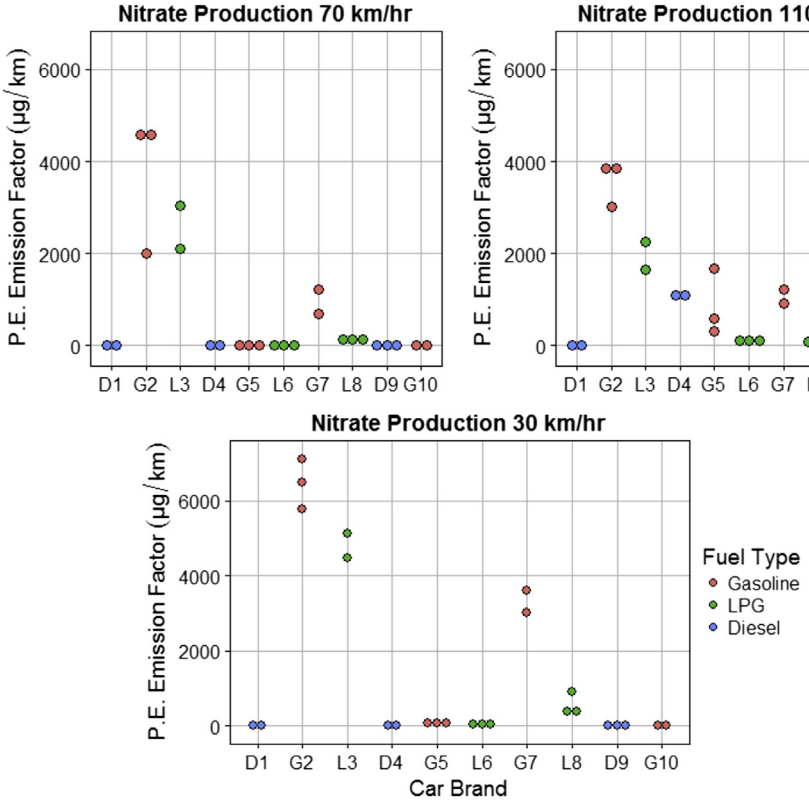

Fig. 2. Aerosol nitrate P.E. emission factors (µg/km) as a function of car brand and speed. Individual measurements are represented by dots.

Inconsistent patterns of aerosol nitrate production, as a function of speed, were observed between the different vehicles tested (Fig. 2). The highest aerosol nitrate production rates were measured from some vehicles (e.g. G5 and G10) at the highest speeds (110 km/h) when the highest values for NO_x were also observed (Fig. S8). However, other vehicles (e.g. G2 and L3) produced the most aerosol nitrate at the lowest tested speed (30 km/h). Although we observe variability in secondary inorganic aerosol production with speed across the different car brands, we do not observe any consistent trends.

Fig. 4 shows a comparision between secondary nitrate production rate and NO, NO_2 and NH_3 emissions for three vehicles of the same brand - D1, G2, and L3 (i.e. Brand A) – that spanned the different fuel types.

Emissions of NH_3 from G2 (gasoline) and L3 (LPG fuel) were much higher than emissions of NO or NO_2. In contrast, emissions of NH_3 were below the detection limit for D1. Elevated emissions of NH_3 from gasoline vehicles have been reported many times in the past (Liu et al., 2015; Livingston et al., 2009; Nowak et al., 2012; Suarez-Bertoa et al., 2014). Vehicles previously reported to emit high levels of NH_3 were medium-duty gasoline fueled vehicles that also emit high CO (Livingston et al., 2009). Here we present

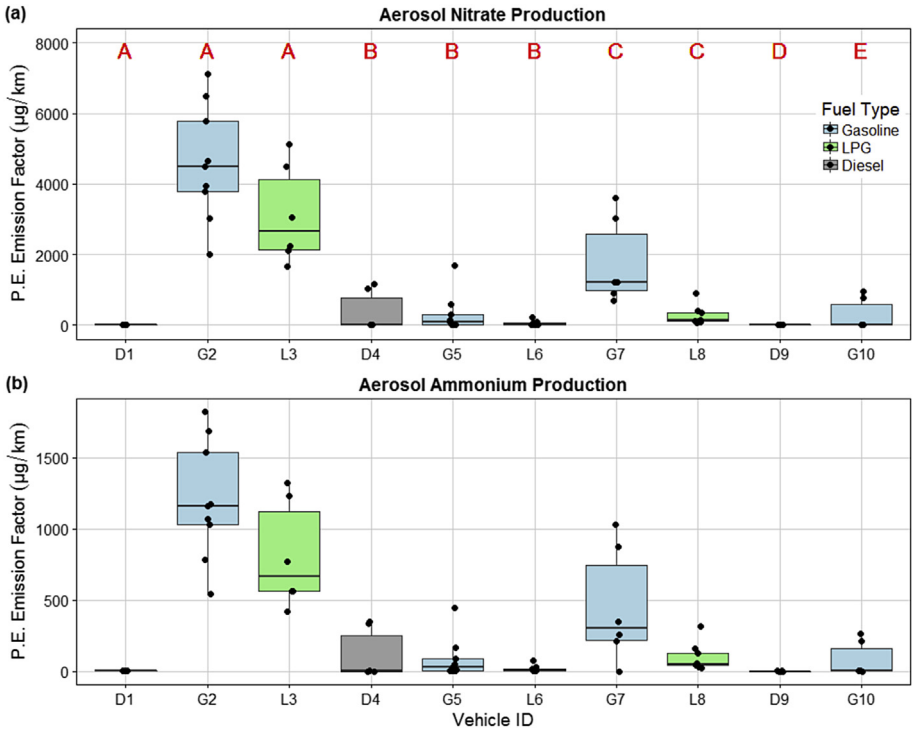

Fig. 3. Secondary (a) aerosol nitrate and (b) aerosol ammonium P.E. emission factors (µg/km) as a function of vehicle ID and colored by fuel type. Additionally, car brand is indicated by the red letters in the top panel corresponding to the corresponding vehicle ID it is above on the x-axis. The edges of the boxplots represent the 25th and 75th quartiles and the whiskers represent the 10th and 90th quartiles. Individually measured data points are shown as black dots. (For interpretation of the references to colour in this figure legend, the reader is referred to the web version of this article.)

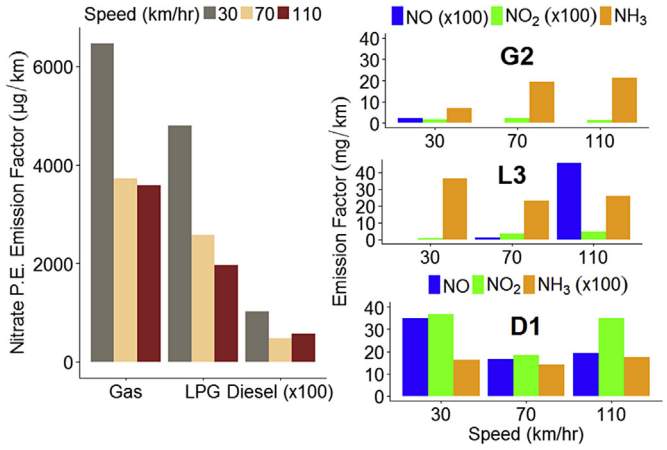

Fig. 4. The (a) production rate of secondary aerosol nitrate from vehicles D1 (×100), G2, and L3 is shown as a function of speed and compared to (b) the emission rates of NO, NO_2, and NH_3 from the different vehicles as a function of speed (NO and NO_2 emission rates are multiplied by 100 for G2 and L3; emission rates of NH_3 are multiplied by 100 for D1).

additional evidence that vehicles fueled by LPG can also emit NH_3 at similar levels as gasoline fueled vehicles. L3 also shows this pattern of high CO emission coupled with high NH_3 emission. Observations from previous studies show that high levels of CO and NH_3 are most often co-emitted when an engine is running under rich-fuel conditions (Bishop et al., 2010; Heeb et al., 2006; Huai et al., 2003). The absence of the three-way catalyst in the diesel vehicles in this study explains why NH_3 emission was not observed for D1.

3.2. Vehicle fuel types and implications for air quality

We observe a direct relationship between the formation of NH_4NO_3 secondary aerosol and photochemical processing of exhaust from gasoline and LPG vehicles that use TWCs. In the KNU OFR, HNO_3 is formed rapidly when NO_2 reacts with OH. The HNO_3 can then react with NH_3 emitted directly from vehicle exhaust to form NH_4NO_3 aerosol (Meng and Seinfeld, 1996). NH_4NO_3 aerosol formation is limited (i) by NH_3 in the case of diesel vehicles, and (ii) by NO_2 in the case of gasoline and LPG vehicles (Fig. 4). These two regimes of NH_3 and NO_x acting as limiting reagents for NH_4NO_3 formation have been observed in the ambient atmosphere (Aksoyoglu et al., 2016; Petetin et al., 2016). In the San Joaquin Valley of California, NH_3 is more abundant than HNO_3 and limits NH_4NO_3 formation, (Markovic et al., 2014), while in the nearby South Coast Air Basin, local and transported sources of NH_3 may act as the limiting reagents for NH_4NO_3 formation (Fraser and Cass, 1998; Nowak et al., 2012). The data presented herein is useful for studying the impact of vehicles on NH_4NO_3 in NO_x- or NH_3-limited regimes (Chen et al., 2016; Mezuman et al., 2016; Petetin et al., 2016). Our results suggest that in an environment in which NH_3 is the limiting reagent for NH_4NO_3 aerosol formation, such as the SMR, (National Institute of Environmental Research, 2015) emission of NH_3 from gasoline and LPG vehicle sources may be a large contributor to local air pollution.

The contribution of on-road gasoline and LPG vehicles to localized NH_4NO_3 production in the SMR depends on many factors including vehicle age (Bishop et al., 2010; Burgard et al., 2006), meteorological conditions influencing mixing and stagnancy (Guo et al., 2014; Liu et al., 2013), driving patterns (Karjalainen et al., 2016; Livingston et al., 2009; Sun et al., 2014), and whether the vehicle is being run under rich-fuel conditions (i.e. low air-to-fuel ratio). The relationship between NH_3 emission, resulting NH_4NO_3

particle formation, and age of the catalyst (i.e. the odometer reading) remains unclear. Previous studies had reported higher NH_3 emission for mid-age (~100,000 km) vehicles that tapered off as vehicle age increased (~200,000 km) (Livingston et al., 2009). This is consistent with the pattern observed here, in which vehicles with the oldest catalysts (G2 and L3) also had the highest NH_4NO_3 production rates. The importance of aggressive stop-and-go driving conditions, characteristic of the SMR, to elevated levels of CO and NH_3 emissions has been reported previously (Bishop et al., 2010; Sun et al., 2014). The quantities and trends reported in this study, however, only reflect emission behavior from constant speed driving conditions, and thus potentially underestimate NH_4NO_3 precursor emissions and subsequent aerosol production. Previous studies have shown emission factors of NH_3 to be higher with more aggressive driving patterns, although the variability in reported emission factors is quite large (Livingston et al., 2009; Suarez-Bertoa et al., 2014). Despite the complex patterns of NH_3 emission from vehicles using TWCs, this study demonstrates that these vehicle emissions have a potential for forming NH_4NO_3 aerosol rapidly and in high yields in response to photochemical perturbation.

A comparison of different NH_3 to CO emission ratios (NH_3:CO) from emission inventories in South Korea and Seoul demonstrates the importance of vehicles as a source of NH_3. From on-road sources in Seoul, annually averaged NH_3:CO emission ratios were 0.024 ppb_v/ppb_v, which is very close to a previously reported on-road emission ratio of 0.031 ± 0.005 ppb_v/ppb_v measured in the South Coast Air Basin (Sun et al., 2014). The calculated NH_3:CO emission ratio from all inventoried sources in Seoul is 0.077 ppb_v/ppb_v suggesting that other sources of NH_3, in addition to on-road vehicle emissions, contribute to NH_3 in the SMR. Although mobile emissions are responsible for approximately 1/4th of the total NH_3 emissions in Seoul, (National Institute of Environmental Research, 2015) a comparison of NO_x and NH_3 emissions (molar quantities) suggest that, since NO_x emissions are ~3.5× larger than NH_3 emissions, NH_4NO_3 formation in Seoul may be limited by the abundance of NH_3. Because on-road vehicles are described as important sources of NH_3 to urban areas in some studies (Chang et al., 2015; Li et al., 2006; Liu et al., 2015), but unimportant in others (Saylor et al., 2010; Yao et al., 2013), direct measurements of on-road NH_3 (e.g. Sun et al., 2014) are necessary for constraining the role of on-road gasoline and LPG vehicles as a NH_3 sources in the SMR. Aircraft measurements have related observed enhancements of NH_4^+ (factor of ~4) above background levels in the South Coast Air Basin to elevated inputs of NH_3 from mobile sources downwind of the Los Angeles urban core (Nowak et al., 2012). These studies and the work described herein suggest that inputs of NH_3 from mobile sources are important to the formation of NH_4NO_3 in the SMR.

These experiments suggest that the chemical reactions that produce NH_3 in TWCs substantially increases the NH_3 available for formation of NH_4NO_3 aerosol. In the face of increasing vehicular emissions of NH_3, continued decreases in domestic emissions of sulfur dioxide (SO_2) would suppress $(NH_4)_2SO_4$ formation, and increase the availability of NH_3 for the formation of NH_4NO_3 (Lee et al., 2004). Further, adoption of selective catalyst reduction systems for NO_x emissions control from diesel vehicles would add more vehicular NH_3 to the SMR, enhancing NH_4NO_3 production (Li et al., 2016; Suarez-Bertoa and Astorga, 2016b). This study suggests that emission control strategies focused on reducing secondary inorganic aerosol pollution from NH_4NO_3 would be most effective by targeting a reduction of NH_3 from the exhaust of vehicles that have three-way catalyst systems.

Acknowledgements

The authors thank the research scientists at Transportation Pollution Research Center, NIER for their contributions to the success of this work. Additional data processing and analysis was supported by Korea Ministry of Environment as “Climate Change Correspondence Program”. Michael Link gratefully acknowledges support by a National Science Foundation (NSF) East Asia and Pacific Summer Institutes (EAPSI) Fellowship (#1613473) for U.S. Graduate Students.

Appendix A. Supplementary data

Details of the experimental set up, instrumentation, and additional analyses can be found in the supporting information.

Supplementary data related to this article can be found at http://dx.doi.org/10.1016/j.atmosenv.2017.02.031.

References

Aksoyoglu, S., Ciarelli, G., El-Haddad, I., Baltensperger, U., Prévôt, A.S.H., 2016. Secondary inorganic aerosols in Europe: sources and the significant influence of biogenic VOC emissions especially on ammonium nitrate. Atmos. Chem. Phys. Discuss. 1–27. http://dx.doi.org/10.5194/acp-2016-739.

Behera, S.N., Sharma, M., Aneja, V.P., Balasubramanian, R., 2013. Ammonia in the atmosphere: a review on emission sources, atmospheric chemistry and deposition on terrestrial bodies. Environ. Sci. Pollut. Res. 20, 8092–8131. http://dx.doi.org/10.1007/s11356-013-2051-9.

Bishop, G.A., Peddle, A.M., Stedman, D.H., Zhan, T., 2010. On-road emission measurements of reactive nitrogen compounds from three California cities. Environ. Sci. Technol. 44, 3616–3620.

Burgard, D.A., Bishop, G.A., Stedman, D.H., 2006. Remote sensing of ammonia and sulfur dioxide from on-road light duty vehicles. Environ. Sci. Technol. 40, 7018–7022.

Chang, Y.H., Zou, Z., Deng, C.R., Huang, K., Collett Jr., J.L., Lin, J., Zhuang, G.S., 2015. The importance of vehicle emissions as a source of atmospheric ammonia in the megacity of Shanghai. Atmos. Chem. Phys. Discuss. 15, 34719–34763.

Chen, D., Liu, Z., Fast, J., Ban, J., 2016. Simulations of sulfate–nitrate–ammonium (SNA) aerosols during the extreme haze events over northern China in October 2014. Atmos. Chem. Phys. 16, 10707–10724. http://dx.doi.org/10.5194/acp-16-10707-2016.

Chhabra, P.S., Lambe, A.T., Canagaratna, M.R., Stark, H., Jayne, J.T., Onasch, T.B., Davidovits, P., Kimmel, J.R., Worsnop, D.R., 2015. Application of high-resolution time-of-flight chemical ionization mass spectrometry measurements to estimate volatility distributions of α-pinene and naphthalene oxidation products. Atmos. Meas. Tech. 8, 1–18. http://dx.doi.org/10.5194/amt-8-1-2015.

Choi, J.C., Lee, M., Chun, Y., Kim, J., Oh, S., 2001. Chemical composition and source signature of spring aerosol in Seoul, Korea. J. Geophys. Res. Atmos. 106, 18067–18074. http://dx.doi.org/10.1029/2001JD900090.

DeCarlo, P.F., Kimmel, J.R., Trimborn, A., Northway, M.J., Jayne, J.T., Aiken, A.C., Gonin, M., Fuhrer, K., Horvath, T., Docherty, K.S., et al., 2006. Field-deployable, high-resolution, time-of-flight aerosol mass spectrometer. Anal. Chem. 78, 8281–8289.

Fraser, M.P., Cass, G.R., 1998. Detection of excess ammonia emissions from in-use vehicles and the implications for fine particle control. Environ. Sci. Technol. 32, 1053–1057.

Friedman, B., Brophy, P., Brune, W.H., Farmer, D.K., 2016. Anthropogenic sulfur perturbations on biogenic oxidation: SO2 additions impact gas-phase OH oxidation products of α- and β-pinene. Environ. Sci. Technol. 50, 1269–1279. http://dx.doi.org/10.1021/acs.est.5b05010.

Geng, H., Ryu, J.Y., Maskey, S., Jung, H.-J., Ro, C.-U., 2011. Characterisation of individual aerosol particles collected during a haze episode in Incheon, Korea using the quantitative ED-EPMA technique. Atmos. Chem. Phys. 11, 1327–1337. http://dx.doi.org/10.5194/acp-11-1327-2011.

Grenoble, D.C., Estadt, M.M., Ollis, D.F., 1981. The chemistry and catalysis of the water gas shift reaction. J. Catal. 67, 90–102. http://dx.doi.org/10.1016/0021-9517(81)90263-3.

Guo, S., Hu, M., Zamora, M.L., Peng, J., Shang, D., Zheng, J., Du, Z., Wu, Z., Shao, M., Zeng, L., et al., 2014. Elucidating severe urban haze formation in China. Proc. Natl. Acad. Sci. 111, 17373–17378.

Heeb, N.V., Forss, A.-M., Brühlmann, S., Lüscher, R., Saxer, C.J., Hug, P., 2006. Three-way catalyst-induced formation of ammonia—velocity- and acceleration-dependent emission factors. Atmos. Environ. 40, 5986–5997. http://dx.doi.org/10.1016/j.atmosenv.2005.12.035, 13th International Symposium on Transport and Air Pollution (TAP-2004)13th International Symposium on Transport and Air Pollution (TAP-2004).

Heo, J.-B., Hopke, P.K., Yi, S.-M., 2009. Source apportionment of PM2.5 in Seoul, Korea. Atmos. Chem. Phys. 9, 4957–4971. http://dx.doi.org/10.5194/acp-9-4957-2009.

Huai, T., Durbin, T.D., Miller, J.W., Pisano, J.T., Sauer, C.G., Rhee, S.H., Norbeck, J.M., 2003. Investigation of NH3 emissions from new technology vehicles as a function of vehicle operating conditions. Environ. Sci. Technol. 37, 4841–4847.

Huang, R.-J., Zhang, Y., Bozzetti, C., Ho, K.-F., Cao, J.-J., Han, Y., Daellenbach, K.R., Slowik, J.G., Platt, S.M., Canonaco, F., Zotter, P., Wolf, R., Pieber, S.M., Bruns, E.A., Crippa, M., Ciarelli, G., Piazzalunga, A., Schwikowski, M., Abbaszade, G., Schnelle-Kreis, J., Zimmermann, R., An, Z., Szidat, S., Baltensperger, U., Haddad, I.E., Prévôt, A.S.H., 2014. High secondary aerosol contribution to particulate pollution during haze events in China. Nat. Adv. online Publ. http://dx.doi.org/10.1038/nature13774.

Jathar, S.H., Friedman, B., Galang, A.A., Link, M.F., Brophy, P., Volckens, J., Eluri, S., Farmer, D.K., 2017. Linking load, fuel and emission controls to photochemical production of secondary organic aerosol from a diesel engine. Environ. Sci. Technol. 51.

Karjalainen, P., Timonen, H., Saukko, E., Kuuluvainen, H., Saarikoski, S., Aakko-Saksa, P., Murtonen, T., Bloss, M., Dal Maso, M., Simonen, P., Ahlberg, E., Svenningsson, B., Brune, W.H., Hillamo, R., Keskinen, J., Rönkkö, T., 2016. Time-resolved characterization of primary particle emissions and secondary particle formation from a modern gasoline passenger car. Atmos. Chem. Phys. 16, 8559–8570. http://dx.doi.org/10.5194/acp-16-8559-2016.

Kim, Y.P., 2007. Trend and characteristics of ambient particles in Seoul. Asian J. Atmos. Environ. 1, 9–13.

Kuwayama, T., Collier, S., Forestieri, S., Brady, J.M., Bertram, T.H., Cappa, C.D., Zhang, Q., Kleeman, M.J., 2015. Volatility of primary organic aerosol emitted from light duty gasoline vehicles. Environ. Sci. Technol. 49, 1569–1577.

Lambe, A.T., Ahern, A.T., Williams, L.R., Slowik, J.G., Wong, J.P.S., Abbatt, J.P.D., Brune, W.H., Ng, N.L., Wright, J.P., Croasdale, D.R., Worsnop, D.R., Davidovits, P., Onasch, T.B., 2011. Characterization of aerosol photooxidation flow reactors: heterogeneous oxidation, secondary organic aerosol formation and cloud condensation nuclei activity measurements. Atmos. Meas. Tech. 4, 445–461. http://dx.doi.org/10.5194/amt-4-445-2011.

Lambe, A.T., Chhabra, P.S., Onasch, T.B., Brune, W.H., Hunter, J.F., Kroll, J.H., Cummings, M.J., Brogan, J.F., Parmar, Y., Worsnop, D.R., Kolb, C.E., Davidovits, P., 2015. Effect of oxidant concentration, exposure time, and seed particles on secondary organic aerosol chemical composition and yield. Atmos. Chem. Phys. 15, 3063–3075. http://dx.doi.org/10.5194/acp-15-3063-2015.

Lee, T., Kreidenweis, S.M., Collett Jr., J.L., 2004. Aerosol ion characteristics during the big bend regional aerosol and visibility observational study. J. Air Waste Manag. Assoc. 54, 585–592.

Lee, Y.H., Choi, Y., Ghim, Y.S., 2016. Classification of diurnal patterns of particulate inorganic ions downwind of metropolitan Seoul. Environ. Sci. Pollut. Res. 23, 8917–8928. http://dx.doi.org/10.1007/s11356-016-6125-3.

Li, R., Palm, B.B., Ortega, A.M., Hlywiak, J., Hu, W., Peng, Z., Day, D.A., Knote, C., Brune, W.H., de Gouw, J.A., Jimenez, J.L., 2015. Modeling the radical chemistry in an oxidation flow reactor: radical formation and recycling, sensitivities, and the OH exposure estimation equation. J. Phys. Chem. A 119, 4418–4432. http://dx.doi.org/10.1021/jp509534k.

Li, Y., Schichtel, B.A., Walker, J.T., Schwede, D.B., Chen, X., Lehmann, C.M., Puchalski, M.A., Gay, D.A., Collett, J.L., 2016. Increasing importance of deposition of reduced nitrogen in the United States. Proc. Natl. Acad. Sci. 113 (21), 201525736.

Li, Y., Schwab, J.J., Demerjian, K.L., 2006. Measurements of ambient ammonia using a tunable diode laser absorption spectrometer: characteristics of ambient ammonia emissions in an urban area of New York City. J. Geophys. Res. Atmos. 111.

Link, M.F., Friedman, B., Fulgham, R., Brophy, P., Galang, A., Jathar, S.H., Veres, P., Roberts, J.M., Farmer, D.K., 2016. Photochemical processing of diesel fuel emissions as a large secondary source of isocyanic acid (HNCO). Geophys. Res. Lett. 43 http://dx.doi.org/10.1002/2016GL068207, 2016GL068207.

Liu, T., Wang, X., Deng, W., Zhang, Y., Chu, B., Ding, X., Hu, Q., He, H., Hao, J., 2015. Role of ammonia in forming secondary aerosols from gasoline vehicle exhaust. Sci. China Chem. 58, 1377–1384. http://dx.doi.org/10.1007/s11426-015-5414-x.

Liu, T., Wang, X., Hu, Q., Deng, W., Zhang, Y., Ding, X., Fu, X., Bernard, F., Zhang, Z., Lü, S., et al., 2016. Formation of secondary aerosols from gasoline vehicle exhaust when mixing with SO 2. Atmos. Chem. Phys. 16, 675–689.

Liu, X.G., Li, J., Qu, Y., Han, T., Hou, L., Gu, J., Chen, C., Yang, Y., Liu, X., Yang, T., et al., 2013. Formation and evolution mechanism of regional haze: a case study in the megacity Beijing, China. Atmos. Chem. Phys. 13, 4501–4514.

Livingston, C., Rieger, P., Winer, A., 2009. Ammonia emissions from a representative in-use fleet of light and medium-duty vehicles in the California South Coast Air Basin. Atmos. Environ. 43, 3326–3333. http://dx.doi.org/10.1016/j.atmosenv.2009.04.009.

Markovic, M.Z., VandenBoer, T.C., Baker, K.R., Kelly, J.T., Murphy, J.G., 2014. Measurements and modeling of the inorganic chemical composition of fine particulate matter and associated precursor gases in California's San Joaquin Valley during CalNex 2010. J. Geophys. Res. Atmos. 119 http://dx.doi.org/10.1002/2013JD021408, 2013JD021408.

Meng, Z., Seinfeld, J.H., 1996. Time scales to achieve atmospheric gas-aerosol equilibrium for volatile species. Atmos. Environ. 30, 2889–2900.

Mezuman, K., Bauer, S.E., Tsigaridis, K., 2016. Evaluating secondary inorganic aerosols in three dimensions. Atmos. Chem. Phys. 16, 10651–10669. http://dx.doi.org/10.5194/acp-16-10651-2016.

Middlebrook, A.M., Bahreini, R., Jimenez, J.L., Canagaratna, M.R., 2012. Evaluation of composition-dependent collection efficiencies for the Aerodyne aerosol mass spectrometer using field data. Aerosol Sci. Technol. 46, 258–271. http://dx.doi.org/10.1080/02786826.2011.620041.

Ministry of Land, Infrastructure, and Transport, 2016. Total Registered Motor Vehicles.

National Institute of Environmental Research, 2015. 2013 National Air Pollutants Emission Inventory.

Nordin, E.Z., Eriksson, A.C., Roldin, P., Nilsson, P.T., Carlsson, J.E., Kajos, M.K., Hellén, H., Wittbom, C., Rissler, J., Löndahl, J., Swietlicki, E., Svenningsson, B., Bohgard, M., Kulmala, M., Hallquist, M., Pagels, J.H., 2013. Secondary organic aerosol formation from idling gasoline passenger vehicle emissions investigated in a smog chamber. Atmos. Chem. Phys. 13, 6101–6116. http://dx.doi.org/10.5194/acp-13-6101-2013.

Nowak, J.B., Neuman, J.A., Bahreini, R., Middlebrook, A.M., Holloway, J.S., McKeen, S.A., Parrish, D.D., Ryerson, T.B., Trainer, M., 2012. Ammonia sources in the California South Coast Air Basin and their impact on ammonium nitrate formation. Geophys. Res. Lett. 39 http://dx.doi.org/10.1029/2012GL051197. L07804.

Ortega, A.M., Day, D.A., Cubison, M.J., Brune, W.H., Bon, D., de Gouw, J.A., Jimenez, J.L., 2013. Secondary organic aerosol formation and primary organic aerosol oxidation from biomass-burning smoke in a flow reactor during FLAME-3. Atmos. Chem. Phys. 13, 11551–11571.

Park, S.-S., Jung, S.-A., Gong, B.-J., Cho, S.-Y., Lee, S.-J., 2013. Characteristics of PM2. 5 haze episodes revealed by highly time-resolved measurements at an air pollution monitoring supersite in Korea. Aerosol Air Qual. Res. 13, 957–976.

Peng, Z., Day, D.A., Ortega, A.M., Palm, B.B., Hu, W., Stark, H., Li, R., Tsigaridis, K., Brune, W.H., Jimenez, J.L., 2016. Non-OH chemistry in oxidation flow reactors for the study of atmospheric chemistry systematically examined by modeling. Atmos. Chem. Phys. 16, 4283–4305. http://dx.doi.org/10.5194/acp-16-4283-2016.

Peng, Z., Day, D.A., Stark, H., Li, R., Lee-Taylor, J., Palm, B.B., Brune, W.H., Jimenez, J.L., 2015. HOx radical chemistry in oxidation flow reactors with low-pressure mercury lamps systematically examined by modeling. Atmos. Meas. Tech. 8, 4863–4890. http://dx.doi.org/10.5194/amt-8-4863-2015.

Petetin, H., Sciare, J., Bressi, M., Gros, V., Rosso, A., Sanchez, O., Sarda-Estève, R., Petit, J.-E., Beekmann, M., 2016. Assessing the ammonium nitrate formation regime in the Paris megacity and its representation in the CHIMERE model. Atmos. Chem. Phys. 16, 10419–10440. http://dx.doi.org/10.5194/acp-16-10419-2016.

Saylor, R.D., Edgerton, E.S., Hartsell, B.E., Baumann, K., Hansen, D.A., 2010. Continuous gaseous and total ammonia measurements from the southeastern aerosol research and characterization (SEARCH) study. Atmos. Environ. 44, 4994–5004. http://dx.doi.org/10.1016/j.atmosenv.2010.07.055.

Shin, H.J., Kim, J.C., Lee, S.J., Kim, Y.P., 2012. Evaluation of the optimum volatile organic compounds control strategy considering the formation of ozone and secondary organic aerosol in Seoul, Korea. Environ. Sci. Pollut. Res. 20, 1468–1481. http://dx.doi.org/10.1007/s11356-012-1108-5.

Suarez-Bertoa, R., Astorga, C., 2016a. Isocyanic acid and ammonia in vehicle emissions. Transp. Res. Part Transp. Environ. 49, 259–270. http://dx.doi.org/10.1016/j.trd.2016.08.039.

Suarez-Bertoa, R., Astorga, C., 2016b. Unregulated emissions from light-duty hybrid electric vehicles. Atmos. Environ. 136, 134–143.

Suarez-Bertoa, R., Zardini, A.A., Astorga, C., 2014. Ammonia exhaust emissions from spark ignition vehicles over the new European driving cycle. Atmos. Environ. 97, 43–53.

Suarez-Bertoa, R., Zardini, A.A., Lilova, V., Meyer, D., Nakatani, S., Hibel, F., Ewers, J., Clairotte, M., Hill, L., Astorga, C., 2015. Intercomparison of real-time tailpipe ammonia measurements from vehicles tested over the new world-harmonized light-duty vehicle test cycle (WLTC). Environ. Sci. Pollut. Res. 22, 7450–7460. http://dx.doi.org/10.1007/s11356-015-4267-3.

Sun, K., Tao, L., Miller, D.J., Khan, M.A., Zondlo, M.A., 2014. On-road ammonia emissions characterized by mobile, open-path measurements. Environ. Sci. Technol. 48, 3943–3950.

Tkacik, D.S., Lambe, A.T., Jathar, S., Li, X., Presto, A.A., Zhao, Y., Blake, D., Meinardi, S., Jayne, J.T., Croteau, P.L., Robinson, A.L., 2014. Secondary organic aerosol formation from in-use motor vehicle emissions using a potential aerosol mass reactor. Environ. Sci. Technol. 48, 11235–11242. http://dx.doi.org/10.1021/es502239v.

Wang, G., Zhang, R., Gomez, M.E., Yang, L., Zamora, M.L., Hu, M., Lin, Y., Peng, J., Guo, S., Meng, J., Li, J., Cheng, C., Hu, T., Ren, Y., Wang, Y., Gao, J., Cao, J., An, Z., Zhou, W., Li, G., Wang, J., Tian, P., Marrero-Ortiz, W., Secrest, J., Du, Z., Zheng, J., Shang, D., Zeng, L., Shao, M., Wang, W., Huang, Y., Wang, Y., Zhu, Y., Li, Y., Hu, J., Pan, B., Cai, L., Cheng, Y., Ji, Y., Zhang, F., Rosenfeld, D., Liss, P.S., Duce, R.A., Kolb, C.E., Molina, M.J., 2016. Persistent sulfate formation from london fog to chinese haze. Proc. Natl. Acad. Sci. 113, 13630–13635. http://dx.doi.org/10.1073/pnas.1616540113.

Wang, Y., Yao, L., Wang, L., Liu, Z., Ji, D., Tang, G., Zhang, J., Sun, Y., Hu, B., Xin, J., 2013. Mechanism for the formation of the January 2013 heavy haze pollution episode over central and eastern China. Sci. China Earth Sci. 57, 14–25. http://dx.doi.org/10.1007/s11430-013-4773-4.

Yao, X., Hu, Q., Zhang, L., Evans, G.J., Godri, K.J., Ng, A.C., 2013. Is vehicular emission a significant contributor to ammonia in the urban atmosphere? Atmos. Environ. 80, 499–506. http://dx.doi.org/10.1016/j.atmosenv.2013.08.028.